Combinatorial Selection and Binding of Phosphorothioate Aptamers Targeting Human NF-κB RelA(p65) and p50†

David J. King,‡,§ Suzanne E. Bassett,‡,§ Xin Li,§ Susan A. Fennewald,|| Norbert K. Herzog,|| Bruce A. Luxon,§ Robert Shope,|| and David G. Gorenstein*,§

Department of Human Biological Chemistry and Genetics and Sealy Center for Structural Biology and Department of Pathology and WHO Collaborating Center for Tropical Diseases, University of Texas Medical Branch, Galveston, Texas 77555

Received March 20, 2002

ABSTRACT: Previously, we reported the in vitro combinatorial selection of phosphorothioate aptamers or "thioaptamers" targeting the transcription factor NF-IL6. Using the same approach and purified recombinant human NF-κB proteins RelA(p65) and p50, duplex thioaptamers have been selected that demonstrate high-affinity, competitive binding with the duplex 22-mer binding site, IgκB. Binding energetics of RelA-(p65) and p50 homodimers were studied using a quantitative electrophoretic mobility shift assay or EMSA. As a reference system for competitive aptamer binding, the duplex 22-mer phosphoryl binding site known as Igκ was determined to bind each p65 and p50 homodimer with a 1:1 stoichiometry and with affinities, determined by global analysis, $K_d = 4.8 \pm 0.2$ nM for p65 and $K_d = 0.8 \pm 0.2$ nM for p50. A global analysis tool for competitive NF-κB/Igκ binding was developed and utilized to measure the affinity of thioaptamers selected by both p65 and p50. The competition results indicate that the thioaptamers bind and compete for the same NF-κB site as the known promoter element IgκB ($K_d = 78.9 \pm 1.9$ nM for a p65-selected aptamer and 19.6 ± 1.3 nM for a p50-selected thioaptamer). Qualitative gel shift binding experiments with p50 also demonstrate that the nature of enhanced affinity and specificity can be attributed to the presence of sulfur. Collectively, these results demonstrate the feasibility of the thioaptamer in vitro combinatorial selection technology as a method for producing specific, high-affinity ligands to proteins.

The use of oligonucleotides as inhibitors to normal protein function in cells has many advantages. First, primary structure complexity of nucleic acids can be achieved easily using a wide range of enzymatic and chemical synthesis techniques (*1*). Furthermore, chemical modifications, such as the phosphorothioate, can be employed to render the molecules more stable to nucleases (*2*). One of the greatest advantages is that their potential size and complexity can confer a degree of specificity and affinity that the small molecule, noncovalent inhibitors cannot (*3*). The advent of aptamer selection technology has made the discovery of such ligands practical and widespread.

In vitro RNA aptamer combinatorial selection technology was introduced in 1990 by Tuerk and Gold targeting the bacteriophage T4 DNA polymerase (*4*). At the same time, Ellington and Szostak discovered that RNA aptamers could be selected for binding to lower molecular weight organic compounds, suggesting the possibility of catalytic RNAs if selection was performed with transition state analogues (*5*, *6*). The potential of aptamers has been demonstrated with major progress in the past decade. These are impressive diagnostic tools, potential therapeutics and also informative regarding the nature of nucleic acid structure (*7*, *8*). The technology has been extended to DNA and RNA, both single and double stranded, as well as to DNA containing a variety of modifications, largely through postselection modifications (*5*, *6*). Aptamer technology has been applied to different targets including whole viruses, proteins, peptides, amino acids, and biological cofactors, showing that aptamers can be developed for any desired molecule regardless of its complexity (*1*, *7*).

A randomized nucleic acid or "aptamer" library can be thought of as a population of many three-dimensional structures, some of which, by virtue of their shape, interact specifically with a target molecule. When one considers transcription factor and DNA duplex aptamer binding, the structural reasons for affinity are still unclear despite impressive structural biology gains over the past 15 years. All transcription factors will bind nonspecific DNA duplexes to some degree. Thus when targeting transcription factors, the highest degree of selectivity is desired. We may utilize quantitative binding data to effectively measure the effect of differences in aptamer sequence, thus telling us which modifications produce tighter binding, more specific agents. This is especially important in the case of NF-κB[1] where dimers of the same family have subtle differences in sequence preference. Only a single base change in a given duplex can alter the affinity in gel shift experiments.

† This work was funded in part by NIEHS Grant ES06676, Welch Foundation Grant H1296, NIH Grant AI27744, and DARPA Grant 9624-107FP.

* To whom correspondence should be addressed. Phone: (409) 747-6800. Fax: (409) 747-6850. E-mail: david@nmr.utmb.edu.

‡ These authors contributed equally to this work.

§ Department of Human Biological Chemistry and Genetics and Sealy Center for Structural Biology.

|| Department of Pathology and WHO Collaborating Center for Tropical Diseases.

[1] Abbreviations: NF-IL6, nuclear factor interleukin 6; NF-κB, nuclear factor kappa B; EMSA, electrophoretic mobility shift assay.

10.1021/bi020220k CCC: $22.00
Published on Web 07/04/2002

NF-κB was first discovered to bind to a 10 base pair region of the κ light chain gene enhancer in pre-B lymphocytes (*9*). NF-κB dimers are inducible transcription factors, which exist in the cytoplasm in an inactivated state associated with an inhibitor protein, IκB. IκB masks NF-κB's nuclear localization sequence and inhibits NF-κB's translocation to the cell nucleus. A variety of stimuli have been reported to activate NF-κB, including phorbol esters, UV irradiation, growth factors and cytokines, viral infection, and LPS (*10*). Upon activation, NF-κB translocates to the nucleus where it influences transcription of genes involved in the inflammatory and immune responses, as well as developmental processes and metabolic enzymes governing normal cell homeostasis.

Although a κB consensus sequence [GGG(R)NN(Y)(Y)-CC] has been established (*11*), the binding specificity of any given NF-κB dimer is determined by the two subunits which comprise it (*12*). The mammalian NF-κB family of transcription factors includes RelA(p65), c-Rel, RelB, p50/p105, and p52/p100 (*13*). ATP-dependent cleavage of the larger, inhibitory proteins p100 and p105 is necessary for the production of p52 and p50, respectively (*14*). NF-κB proteins are related through the presence of a Rel homology region (RHR) that contains approximately 300 conserved N-terminal amino acids (*10*, *15*). The RHR is necessary for DNA binding, protein dimerization, and interactions with IκB proteins. The RHR also contains the nuclear localization sequence (NLS) that is necessary for the translocation of NF-κB proteins to the nucleus (*10*). The inhibitory IκB proteins, such as the NF-κB DNA binding proteins, also exhibit a great degree of diversity, including IκB-α, IκB-*β*, IκB-*δ*, IκB-*ϵ*, IκB-*γ*, p105, p100, and Bcl-3 in vertebrates. Disruption of NF-κB genes using transgenic technology leads to deficiencies in immune responses. Although developmentally normal, mice deficient in p50 display functional defects in immune responses (*16*). Disruption of the p65 locus leads to embryonic lethality at 15−16 days of gestation, concomitant with a massive degeneration of the liver by programmed cell death or apoptosis (*16*). Mice cells lacking p65 are defective in the stimulus-induced transcription of TNF-α, IκB-α, and granulocyte−macrophage colony stimulating factor (GM-CSF) (*16*). In addition, lymphocytes from p65 knockouts show reduced proliferative response upon stimulation (*17*). Collectively, knockout mice have demonstrated the importance of NF-κB proteins in immune system function. NF-κB is therefore an obvious target for new types of anti-inflammatory and immunomodulating treatments. Current antiinflammatory treatments include glucocorticoids (*18*), anti-oxidants (*19*), and gliotoxin, a naturally occurring inhibitor of NF-κB (*20*). All of these treatments have their issues of selectivity, effectiveness, and toxicity, and prolonged inhibition of NF-κB, given the data from single and double knockout mouse studies, is inappropriate (*16*, *17*).

Aptamers are typically generated using an iterative process called in vitro selection, which requires a purified target molecule and a nucleic acid library. The iterative process involves mixing the target and the library in known ratios and separating the bound members of the library from the unbound. The bound fractions are then amplified using PCR, and the process is repeated until the population is sufficiently enhanced for high-affinity aptamers. Typically, the random library will converge to only a few, high-affinity sequence families producing suitable compounds for further study. Kunsch et al., using in vitro selection techniques, have determined that homodimers of NF-κB p65 can select and bind DNA sequences that NF-κB p50 homodimers do not bind (*11*). Using purified recombinant p50, p65, and c-Rel proteins, they showed that optimal, dimer-specific DNA binding motifs can be selected from a pool of random, normal backbone oligonucleotides. These results, however, were determined qualitatively, and the actual energetic differences in binding were not determined.

An important class of backbone-modified nucleic acids includes the phosphorothioates where either one (monothio) or two (dithio) nonbridging oxygens are replaced with sulfur atoms. Their most basic attributes include enhanced nuclease resistance (*21*), the ability to interact with enhanced specificity to proteins (*22*, *23*), and the ability to form complementary base pairs with both DNA and RNA (*24*). This work focuses on monothiophosphate DNA duplexes, their ability to interact with proteins, and their development in the field of aptamer technology. The phosphorothioate and phosphorodithioate backbone modifications are not only nuclease resistant but taken up efficiently by cells. Unlike the dithiophosphates, which are achiral at each phosphorus center, the monothiophosphates introduce a new chiral center at each phosphorus position. Nucleotides containing the phosphorothioate S_p configuration can be incorporated into combinatorial DNA libraries by *Taq* DNA polymerase to produce phosphorothioate modifications containing the R_p configuration (*25*−*28*).

Previously, we reported the methods for novel combinatorial selection of chiral phosphorothioate, enhanced nuclease-resistant aptamers for the transcription factor NF-IL6 (*27*). In this paper, we present the combinatorial selection and quantitative binding analysis of thioaptamers selected for both the p50 and p65 NF-κB homodimers. The basis for enhanced binding of these thioaptamers to proteins has been attributed to altered ion affinities (*29*). Because sulfur interacts less favorably with hard cations such as Na^+, the thio-substituted phosphate esters then act as bare anions, and since energy is not required to strip the cations from the backbone, phosphorothioates should bind even tighter to proteins. It has been shown that as much as 1 kcal/mol of binding energy between an enzyme and a phosphorothioate substrate can be detected when one changes from the R_p to the S_p configuration about phosphorus. This demonstrates the very specific nature of protein and phosphorothioate DNA interactions (*30*−*33*). Sulfur also has a much larger van der Waals radius than oxygen. These bulky effects can change the torsional angles of the nucleic acid backbone. Smith and Nikonowicz (*34*) have investigated the RNA binding site of the MS2 capsid using NMR spectroscopy, and they find that phosphorothioate substitution causes an unpaired adenine necessary for formation of the MS2 capsid protein−RNA complex to loop out of the RNA helix into the major groove.

Oligonucleotides possessing high thiophosphate backbone substitutions appear to bind nonspecifically to proteins relative to normal phosphate esters. Thus, there has been a need to optimize the total number of thioated phosphates using either rational design principles or combinatorial techniques to decrease nonspecific binding to nontarget proteins in the cell and enhance only the specific favorable interactions with a target such as NF-κB. Our results suggest

that the selection can be employed to obtain protein-specific thioaptamers. We report that the presence of thioates in the aptamer backbone confers increased affinity and specificity for target NF-κB dimers. The quantitative approach reported here is essential to understanding the forces of phosphorothioate interaction with NF-κB.

MATERIALS AND METHODS

NF-κB Expression and Purification. Human NF-κB GST fusion proteins, p65 and p50, were expressed in *Escherichia coli* BL21 using the pGEX vector (Pharmacia). The NF-κB constructs contain the sequences for residues 12−317 of human p65 and 11−400 of human p50. These fragments include the conserved Rel homology regions, or RHR's, of NF-κB. Their calculated masses of p65 and p50 monomers are 34842 and 46072 Da, respectively. Bacteria were grown in LB at 37 °C until the OD_{600} reached 0.5 when 1 mM IPTG was added to a 20 L fermentor. The induction continued for 4 h. The cells were harvested by centrifugation and then resuspended in 20 mM NaH_2PO_4, pH 7, 1 M NaCl, 1 mM EDTA, 1 mg/mL aprotinin, and 1 mM PMSF. Lysozyme was then added to the suspension to a final concentration of 1 mg/mL, followed by three freeze/thaw cycles with sonication. The lysate was then centrifuged to pellet the debris at 10000*g*, and the soluble fraction was loaded directly onto a 25 mm/45 cm glutathione−Sepharose affinity column equilibrated with lysis buffer. The column was washed with the high salt lysis buffer to remove contaminating bacterial nucleic acids and proteins. The UV spectrum was monitored until absorbance at all wavelengths reached a baseline. The column was then washed with the same buffer containing 100 mM NaCl in preparation for thrombin cleavage. One thousand units of thrombin was then loaded onto the affinity column and allowed to incubate overnight at 4 °C. The cleaved, eluted protein was concentrated to 10 mL and loaded onto a Mono Q anion-exchange column, 25 mm/200 cm. The NF-κB proteins did not bind to this column, and the flow through was collected. The protein was then concentrated and quantified by UV spectroscopy and Coomassie staining (Bio-Rad). Both quantification methods yielded the same result within 10%. This produces soluble and active protein that is greater than 99% pure as estimated by 4−20% gradient SDS−PAGE, UV spectral analysis, and MALDI TOF.

Combinatorial Selection of Thioaptamers. The methods for combinatorial selection of thioaptamers using targeting p65 and p50 are essentially the same as the methods described for NF-IL6 (*27*). Briefly, a 66-mer single-stranded library was chemically synthesized containing a 22-base random or variable region flanked by 19-base 5′ and 21-base 3′ primer segments: 5′ ATGCTTCCACGAGCCTTTC N_{22} CTGCGAGGCGGTAGTCTATTC 3′. The single-stranded library was replicated using Klenow fragment DNA polymerase and subsequently amplified using *Taq* polymerase and a mixture of 40 μM each dATP(αS), dTTP, dGTP, and dCTP, 500 μM $MgCl_2$, 2.9 μM 66-mer random template, 0.5 unit of *Taq* polymerase, and 400 nM each primer in a total volume of 100 μL. PCR is run for 25−35 cycles of 95 °C/1 min, 55 °C/1 min, and 68 °C/1 min. The resulting 66-mer library, therefore, contained R_p configured monothiophosphate modification 5′ to every dA residue, including those residues in the primer regions. Purified recombinant NF-κB proteins were used to select thioaptamers using the filter binding method (*35*) until the libraries converged with 20 iterations (p65) and 15 iterations (p50). The PCR-amplified random library of the chiral duplex phosphorothioate 66-mer at dA positions (100 pmol) was incubated with 10 pmol of NF-κB p50 or p65 in 50 μL of buffer containing 10 mM Tris, pH 7.5, 1 mM DTT, and 50−400 mM KCl and filtered through Millipore HAWP 25 mm nitrocellulose filters (following a modification of the protocol from ref *35*). Under these conditions the DNA−protein complexes were retained on the filter. The filters had been previously presoaked in 10 mM Tris, pH 7.5, 1 mM DTT, and 50−400 mM KCl, 1× binding buffer that contains no protein or DNA. The filter was then washed with 10 mL of 1× binding buffer to remove the majority of the DNA, which only weakly bound to the protein. A 1 mL solution of 8 M urea and 4 M NaCl was then added to elute the protein-bound DNA. A negative control without protein was performed simultaneously to monitor any nonspecific binding of the thiophosphate DNA library to the nitrocellulose filter. The DNA was ethanol-precipitated and once again PCR-amplified with the dATP(αS) nucleotide mix. The PCR products were analyzed by 15% nondenaturing polyacrylamide gel electrophoresis.

Refolding of p65. Maximum purity from contaminating bacterial nucleic acids is essential for the quantitative analysis of binding. To ensure this, a sample of p65 was treated as follows. The p65 protein was purified as described above; however, it was then unfolded in 10000 MWCO dialysis cassettes (Pierce) in buffer with 7 M urea and 14.3 mM β-mercaptoethanol. This material was then loaded onto a Mono S FPLC column at 2 mL/min until the absorbance reached a baseline. Under these conditions, it is assumed that any remaining bacterial nucleic acid potentially bound to the protein will flow through the column and only the positively charged, denatured protein will bind to the cation-exchange resin. Thus, no competing, trace amounts of contaminant will significantly alter the apparent binding affinity. A linear gradient (0−1 M NaCl) was then applied, and p65 appears in fractions containing about 300 mM NaCl. The peak fraction was pooled and redialyzed against denaturing buffer to remove salt. The protein was then refolded in normal phosphate buffer described above. Binding to Igκ was performed to compare equilibrium constants (K_d) of natively purified and denatured purified p65.

Oligonucleotides. All oligonucleotides, including PCR primers, were purchased from Midland Certified Reagents, Midland, TX, where they are synthesized by standard phosphoramidite chemistry and purified by reverse-phase HPLC. Each 22-mer Igκ strand used for quantitative binding analysis was labeled separately using T4 polynucleotide kinase and [γ-^{32}P]dATP, followed by removal of the unincorporated nucleotide by gel filtration. The gel filtration products were lyophilized using a speed vac and then resuspended in binding buffer and quantified. The duplex was annealed and its purity assessed on 8% polyacrylamide TBE gels. Table 1 lists the oligonucleotides used in the quantitative binding studies. The combinatorially selected sequences have monothiophosphate modification 5′ to each dA residue since the enzymatic steps of our in vitro selection utilized dATP(αS).

Table 1: Sequences of Oligonucleotides Used in Binding Analysis

Igκ sequence
5′ GCCTGGGAAAGTCCCCTCAACT 3′
3′ CGGACCCTTTCAGGGGAGTTGA 5′
p65-selected[a]
5′ CGGGGTGTTGTCCTGTGCTCTCC 3′
3′ GCCCCACAACAGGACACGAGAGG 5′
p50-selected[a]
5′ GGGGTTCCACCTTCACTGGGCG 3′
3′ CCCCAAGGTGGAAGTGACCCGC 5′

[a] DNA sequences of combinatorially selected thioaptamers, chemically synthesized oligonucleotide duplexes with thiophosphate modification 5′ to each dA residue.

Enzymatic Synthesis of 5′ Biotin-Labeled Phosphorothioate Aptamers. Chiral phosphorothioates were PCR synthesized as previously described (*27*). Oligonucleotides selected combinatorially have monothiophosphate modification 5′ to each dA residue in a 22 base pair randomized segment. The 5′ biotinylated PCR primers for each construct were obtained from Midland Certified Reagents, Midland, TX. PCR is run for 35 cycles with limiting concentrations of plasmid template, obtained by TA cloning of the PCR and selection products, and once again a mix of dATP(αS), dTTP, dCTP, and dGTP. To determine the optimal plasmid DNA concentration for the aptamer synthesis, a serial dilution was performed on the products from a Quiagen miniprep kit. This prevents any significant amount of plasmid DNA in the final aptamer preparation. The PCR products were further purified by filtering over nitrocellulose to remove *Taq* polymerase and concentrated using an Amicon spin microconcentrator.

Electrophoretic Mobility Shift Assay (EMSA). The binding affinity of the NF-κB proteins was analyzed using the electrophoretic mobility shift assay. Native 8% polyacrylamide (135 mm/155 mm/2 mm) gels were prepared using stock solutions of 30% acrylamide, 2% bisacrylamide, 5× TBE, pH 7.6, and 80% glycerol and 30% ammonium persulfate. The 5× TBE contained 445 mM Tris base, 445 mM boric acid, and 10 mM EDTA, pH 7.6. The final conditions of the gel were 0.25× TBE, 8% acrylamide, 0.075% bisacrylamide, 2.5% glycerol, 0.0675% APS, and 0.075% TEMED. The gels were cooled to 4 °C before the binding reactions were loaded. The conditions of the binding reactions were 10 mM KH_2PO_4, 100 mM NaCl, 0.1 mM EDTA, 5 mM $MgCl_2$, 40 mM DTT, 6% glycerol, and 1 mg/mL BSA at pH 7.0.

Both the proteins and the DNA were serially diluted in 30% glycerol and binding buffer, respectively. The reactions were 50 μL total volume consisting of 10 μL of water, 10 μL of a 5× mix containing $MgCl_2$, KH_2PO_4, DTT, NaCl, and BSA, 10 μL of protein and 20 μL of ^{32}P-labeled DNA. In the case of competition experiments, the 10 μL of water was substituted with 10 μL of the preannealed aptamer duplex. Since the aptamer duplex was annealed in 1× binding buffer, the 5× mix was reduced to 4× concentration. For a single isotherm, the protein or aptamer concentration remained fixed, and the 22-mer Igκ duplex DNA was titrated at up to 16 different concentrations in 16 separate tubes. There was a 1 h incubation period before addition of 1 μL of tracking dye and loading onto the gel. For the best resolution of bands, alternate wells of the gel were skipped. Each isotherm was generated using two gels. The gels were run for 60 min at 1 mA/cm^2 until the xylene cyanol and bromophenol blue bands are resolved. The gels were then placed on blotting paper and dried with vacuum at 75 °C heating for 1.5 h. The radioactivity on the gel in counts per minute (cpm) was measured using a Packard Instant Imager.

Analysis of Binding Data. The protein−DNA complex was separated on the gel from the free DNA, and the total radioactivity on the gels is used to determine the specific activity of the DNA. Since the ^{32}P-labeled Igκ DNA is titrated into a fixed amount of NF-κB, a linear regression can be performed to determine the specific activity of the DNA on the gel in moles per counts per minute. The observable, dependent variable in the EMSA is the concentration of DNA bound [DB] and is proportional to the specific activity in moles per counts per minute times the radioactivity in the shifted band (counts per minute shifted) divided by the volume of the reaction loaded on the gel (eq 1). The simple

$$[DB] = [(mol/cpm)(cpm\ shifted)]/volume\ loaded \quad (1)$$

equilibrium expression (eq 2) was used to derive a mathematical model for analysis of [DB] in terms of the two independent variables, Igκ total concentration ([D]t) and NF-κB dimer concentration ([P]t) (eqs 3 and 4). In our

$$K_d = [P][D]/[DB] \quad (2)$$

$$z = [D]t + [P]t + K_d \quad (3)$$

$$[DB] = (z - [(z^2) - 4[D]t[P]t]^{1/2})/2 \quad (4)$$

experiments, each isotherm was collected as a titration where labeled Igκ was titrated into a fixed amount of NF-κB dimer. Thus, we reasoned that the saturation point could also serve as an accurate determination of total active protein ([P]t) if this variable is allowed to float as a calculated parameter. When total protein was allowed to float in the regression, the new value called [P]t* was generated separately for each isotherm at a given NF-κB concentration. These equations are sufficient to analyze data sets with two independent variables and one dependent variable; thus, global fitting of multiple isotherms is possible. The data were globally fit using the known quantities [D]t, as measured by UV spectroscopy, [DB], the amount of DNA in the shifted band on the gel, and [P]t*, as determined by allowing [P]t to float as a parameter. [P]t* approached the measurements of [P]t made by UV and Coomassie staining for protein concentration determination and was found to approximate the concentration of total NF-κB dimer. To investigate the possibility of cooperative interactions between NF-κB monomers, we generated Hill plots of log $[Ig\kappa]_{free}$ versus log fb/(1 − fb), where fb is the fraction of labeled Igκ bound.

To be sure that the aptamers bound to the same NF-κB binding site as Igκ, fixed concentrations of thioaptamer were added to the reference titration of ^{32}P-labeled Igκ. The equations for global competitive inhibition analysis were derived as follows. The model for competitive inhibition is assumed as follows:

$$I + P \overset{K_I}{\rightleftharpoons} PI$$

where eqs 2 and 5 describe the free concentrations and the equilibrium constants governing their distribution. Here the

$$K_I = [P][I]/[PI] \quad (5)$$

phosphorothioate aptamer competes directly for the same NF-κB sites as Igκ. The binding affinity, K_d^{app}, of the protein for its natural substrate is modulated by the expression $1 + [I]/K_I$, where [I] is free inhibitor concentration and K_I is the dissociation constant of the inhibitor. This expression can be substituted directly into the quadratic equations for simple binding (eqs 6 and 7). The concentrations of all species in

$$z = [D]t + [P]t^* + K_d(1 + [I]/K_I) \quad (6)$$

$$[DB] = (z - [(z^2) - 4[D]t[P]t]^{1/2})/2 \quad (7)$$

solution are related by the mass balance equations (eqs 8 and 9), which allows calculation of [I]. [P] or free protein is

$$[I] = [I]t - [PI] \quad (8)$$

$$[PI] = [P]t^* - [P] - [PD] \quad (9)$$

calculated from the equilibrium expression in eq 10, since K_d for the uninhibited reaction is known. The experimentally

$$[P] = K_d^*[PD]/[D]t - [PD] \quad (10)$$

observable quantity [DB] at multiple [I]t and/or [P]t can be used to determine K_I by global regression analysis. For example, using a value of $K_d = 4.77$ nM (p65/Igκ experimentally determined), one calculates the distribution of species for different experimental [I]t concentrations. The individual fits for each isotherm were used to determine [P]t*, the total active dimer concentration and K_d^{app} at each individual [I]t. Thus the global fitting equations are thermodynamically valid and apply directly to the EMSA/^{32}P-label detection system described here. Again, when the global fit is performed, the adjusted [P]t* values from each single isotherm are used. The program used for plotting and data analysis is SigmaPlot (Jandel Scientific).

Chemiluminescent EMSA for Qualitative Assessment of Aptamer Binding. The EMSA conditions are the same as outlined above; however, labeling the PCR primers used to amplify the 22-mer-selected constructs with 5′ biotin allows visualization of bound/free species using the commercially available chemiluminescent "LightShift" kit (Pierce). The concentration of PCR-synthesized thioaptamer DNA was 1 nM and NF-κB protein was 4 nM. Briefly, once the EMSA gel was run, the reaction products were electroblotted from the EMSA gel to Biodyne B modified nylon membrane (Pierce) and developed in kit buffer containing avidin-linked horseradish peroxidase and its chemiluminescent substrate. The membrane was then exposed to X-ray film, which was then digitally scanned using Adobe Photoshop.

RESULTS

Expression and Purification of NF-κB p50 and p65. The Rel homology region of NF-κB contains the DNA binding, dimerization, and nuclear localization signals of the full-length proteins. Previous methods employed to purify both GST p50 and p65 involved the mixing of cell lysates with a suspension of GSH affinity resin. While the SDS−PAGE showed pure protein, the UV spectrum indicated severe contamination with coeluting bacterial nucleic acid. This is evidenced by a strong absorbance maximum near 260 nm resulting in an ~1:2 280/260 ratio. Our newer method, which does not require nucleic acid precipitating agents such as streptomycin sulfate or poly(ethylenimine), utilizes the ability of high salt (1 M NaCl) to disrupt interactions between NF-κB and short pieces of bacterial DNA created by sonication. Our results demonstrate that no contaminants significant enough to offset our binding constants remain in the purified NF-κB. As shown, there is a dramatic difference between the two spectra, indicating that the newer method has removed most, if not all, contaminating DNA (Figure 1). Shown in Figure 2 are the 4−20% gradient SDS−PAGE analyses of both p50 and p65. The proteins migrate on SDS−PAGE gels according to their appropriate sizes. The calculated 280/260 ratios for p50 and p65 can be obtained from a simulation, based on amino acid composition of the proteins, of their respective UV spectra. The expected versus the experimental 280/260 ratio for p65 is 1.36 and 1.60, respectively. For p50, the expected versus the experimental is 1.35 and 1.33. A sample of this p65 was subjected to a further purification step under denaturing conditions to remove any contaminating material and confirm that the

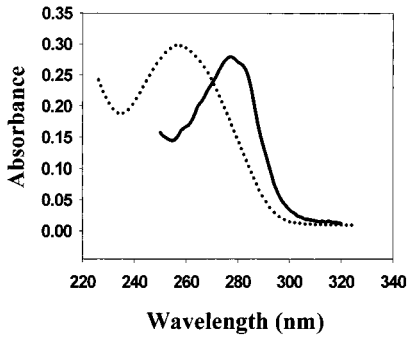

FIGURE 1: Comparison of UV spectra from two different purification schemes: GSH affinity column purified with 1 M NaCl (solid line); GSH affinity column purified with 100 mM NaCl (dotted line).

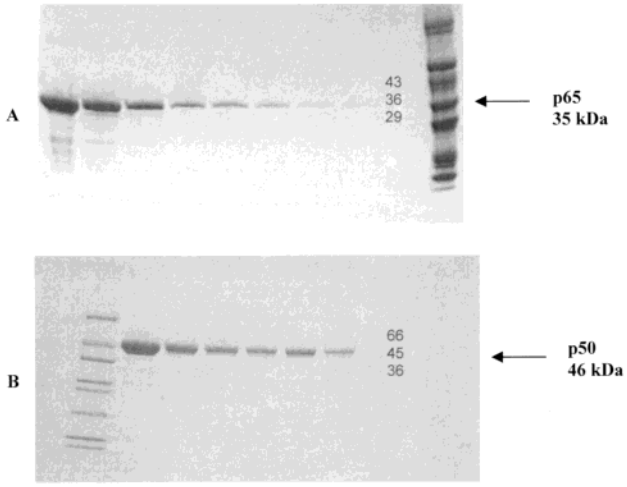

FIGURE 2: Purity of NF-κB proteins p50 and p65. Serial 2-fold dilution of NF-κB proteins on 4−20% gradient reducing SDS−PAGE: (A) p65; (B) p50.

Table 2: DNA Sequencing Results: Monothiophosphate Combinatorial Selection with NF-κB p65

	1	2	3	4	5	6	7	8	9	10	11	12	13	14	15	16	17	18	19	20	21
1	G	G	G	G	T	G	T	T	G	T	C	C	T	G	T	G	C	T	C	T	C
2	G	G	G	G	T	G	T	T	G	T	C	C	T	G	T	G	C	T	C	T	C
3	G	G	G	G	T	G	T	T	G	T	C	C	T	G	T	G	C	T	C	T	C
4	G	G	G	G	T	G	T	T	G	T	C	C	T	G	T	G	C	T	C	T	C
5	G	G	G	G	T	G	T	T	G	T	C	C	T	G	T	G	C	T	C	T	C
6	G	G	G	G	T	G	T	T	G	T	C	C	T	G	T	G	C	T	C	T	C
7	G	G	G	G	T	G	T	T	G	T	C	C	T	G	T	G	C	T	C	T	C
8	G	G	G	G	T	G	T	T	G	T	C	C	T	G	T	G	C	T	C	T	C
9	G	G	G	G	T	G	T	T	C	T	C	C	T	G	T	G	C	T	C	T	C
10	G	G	G	G	T	G	G	T	G	T	G	G	C	G	A	G	G	C	G	G	C
11	G	G	G	G	T	G	G	T	G	T	G	G	C	G	A	G	G	C	G	G	C
12	G	G	G	G	T	G	G	T	G	T	G	G	C	G	A	G	G	C	G	G	C
13	G	G	G	G	T	G	G	T	G	C	G	G	C	G	A	G	G	C	G	G	C
14	G	G	G	G	T	G	T	G	C	T	G	C	T	G	C	G	G	G	C	G	G
15[a]	G	G	A	G	T	A	G	G	T	A	G	G	C	G	A	A	T	T	C	A	G
A[b]	0	0	0	0	0	0	0	0	0	0	0	0	0	0	4	0	0	0	0	0	0
C	0	0	0	0	0	1	0	0	1	C	9	10	C	0	1	0	9	4	10	0	13
G	14	14	14	14	14	13	4	1	13	0	5	4	0	14	0	14	5	1	4	5	1
T	0	0	0	0	0	0	10	13	0	13	0	0	10	0	9	0	0	9	0	9	0
16[c]	G	G	G	G	T	G	T	T	G	T	C	C	T	G	T	G	X	Y	C	T	C

[a] Sequence 15 found to not bind NF-κB p65/p65 in electrophoretic mobility shift assay. [b] Number of times a given residue appears. [c] Consensus sequence based on the residue which appears the majority of the time in this position; note that monothiophospahte modifications are found 5′ to each dA residue on the complementary strand also.

Table 3: DNA Sequencing Results: Monothiophosphate Combinatorial Selection with NF-κB p50

	1	2	3	4	5	6	7	8	9	10	11	12	13	14	15	16	17	18	19	20	21	22
1	G	G	G	A	C	A	C	G	G	C	A	C	A	A	G	A	A	C	A	C	G	G
2	G	G	G	A	C	A	C	G	A	C	A	C	A	A	G	A	A	C	A	C	G	G
3	G	G	G	A	C	A	C	G	G	C	A	C	A	A	G	A	A	C	A	C	A	G
4	G	G	G	A	C	A	C	G	A	C	A	C	A	A	G	A	A	C	A	C	A	G
5	G	G	G	G	C	A	C	G	A	C	A	C	A	A	G	A	A	C	A	C	A	G
6	G	G	G	G	T	T	C	C	A	C	C	T	T	C	A	C	T	G	G	G	C	G
7	G	G	G	G	C	A	G	A	A	C	C	A	T	A	C	A	C	G	G	A	C	G
8	G	C	C	A	C	C	G	C	C	C	C	C	G	A	A	T	C	G	C	A	C	G
9	G	G	G	G	G	T	G	G	C	G	G	T	C	G	A	C	C	T	T	G	T	C
10	G	G	G	A	C	A	C	G	G	C	A	C	A	A	G	A	A	C	A	C	G	G
11	G	G	G	A	C	A	C	G	A	C	A	C	A	A	G	A	A	C	A	C	G	G
12	G	G	G	A	C	A	C	G	G	C	A	C	A	A	G	A	A	C	A	C	A	G
13	G	G	G	A	C	A	C	G	A	C	A	C	A	A	G	A	A	C	A	C	A	G
14	G	G	G	G	C	A	C	G	A	C	A	C	A	A	G	A	A	C	A	C	A	G
15[a]	C	G	A	A	C	G	G	T	G	T	T	G	C	G	T	G	T	T	G	T	T	G
A[b]	0	0	0	9	0	11	0	1	8	0	10	1	10	12	3	11	10	0	10	2	6	0
C	0	1	2	0	12	1	11	2	2	13	3	11	1	1	1	2	3	10	1	10	3	1
G	14	13	12	5	1	0	3	11	4	1	1	0	1	1	10	0	0	3	2	2	4	13
T	0	0	0	0	1	2	0	0	0	0	0	2	2	0	0	1	1	1	1	0	1	0
16[c]	G	G	G	A	C	A	C	G	R	C	A	C	A	A	G	A	A	C	A	C	R	G

[a] Sequence 15 found to not bind NF-κB p50/p50 in electrophoretic mobility shift assay. [b] Number of times a given residue appears. [c] Consensus sequence based on the residue which appears the majority of the time in this position; note that monothiophosphate modifications are found 5′ to each dA residue on the complementary strand also.

equilibrium constant is not offset significantly. The binding results described below indicate that this denaturing protocol for p65 is not necessary. N-Terminal sequencing of the first 10 residues confirms their correct sequences.

Combinatorial Selection of Thioaptamers. Shown in Tables 2 and 3 are the variable region sequences obtained from the p65 and p50 combinatorial selections, respectively. The 66-mer PCR construct used in the selection contains a 22-mer variable region, potentially large enough to have two dimers of NF-κB bound. The consensus sequence at the bottom of each table reveals that the first 10 base pairs contain the 4-base polypurine tract common to normal phosphoryl NF-κB binding sites. The second 5-base half-site reveals differences between thioaptamer selection and selections involving normal phosphate ester backbone DNA; see Discussion. In the next 5−10 base pairs, only very weak NF-κB elements are observed, indicating that the selection could be driven primarily by the presence of the first 5 base pairs, allowing the other half of one NF-κB dimer to select for thio substitutions. In the binding results presented below we observe that, under the conditions of our experiments, there is a 1:1 stoichiometry of a stable NF-κB dimer binding to each aptamer. The sequencing results presented in Table 2 for p65 are truncated by a single base since alignment of the NF-κB binding site or the PCR primer sequence introduced a single base offset. This result is assumed to be a PCR or cloning artifact. The sequences presented in Table 3 for p50 contain all 22 bases of the variable/random region. We have no results suggesting a role for the thiophosphate-modified primer regions; however, it is possible that some

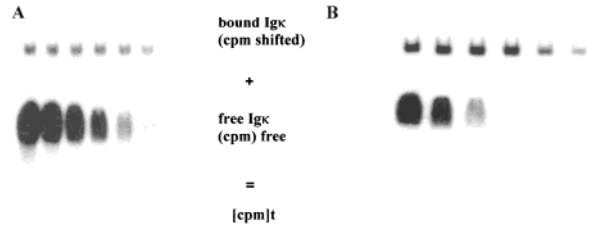

FIGURE 3: EMSA gel for the binding of p65 (A) and p50 (B) to IgκB. A serial 2-fold dilution of the labeled Igκ DNA is made prior to addition to binding reactions. The signals from both bands are added in each lane and are proportional to [DNA]total for each reaction.

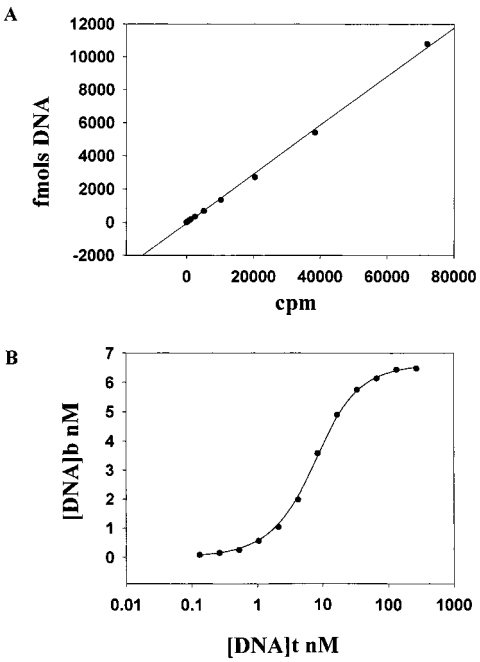

FIGURE 4: EMSA gel analysis. (A) Linear regression analysis to determine the specific activity of IgκB in fmol (*y* axis) per cpm (*x* axis). The slope units of the line are fmol/cpm. (B) Binding isotherm of IgκB or DNA bound vs Igκ total. [p65]t = 5.22 nM ([P]t* = 6.63 ± 0.05 nM); K_d = 4.44 ± 0.194 nM.

weak, nonspecific NF-κB binding occurs in this region. For binding affinity analysis, we selected clone number 1 since it occurred most frequently from the p65 selection and clone 6 from the p50 selection since it demonstrated the tightest binding when initially screened. Sequence number 15 in each table represents a clone from each initial library which failed to bind NF-κB.

Analysis of Binding Data for Igκ: p65 and p50 Homodimers. Figure 3 shows Packard computer images of typical EMSA gels used in these studies for p65 (A) and p50 (B). There appears to be only two species representing bound and free DNA on the gel. This is consistent with the model and stoichiometric ratio that NF-κB binds to the Igκ as a stable dimer, in a 1:1 dimer per 22-mer Igκ duplex. Under the conditions of these experiments, we do not observe any monomer/dimer equilibrium or cooperative interactions between monomers. Figure 4 is the raw data from one titration involving DNA into a fixed concentration of p65 protein. Only six data points are collected from each gel, and the data points representing the lower DNA concentration points are from a separate gel (not shown). The first plot (A) is generated by adding the radioactivity in each lane in

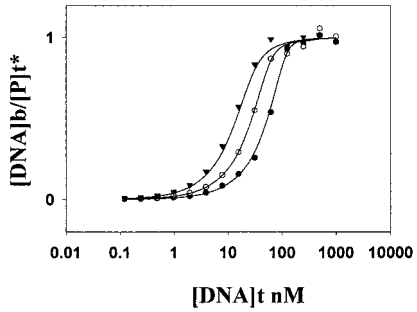

FIGURE 5: Global analysis of binding data for p65: (●) 100 nM pt, (○) 50 nM pt, and (▼) 25 nM pt.

Table 4: Summary of Binding Results for Igκ/NF-κB

	K_d (nM)	R^2
1[a]	4.77 ± 0.21	0.991
2[b]	4.11 ± 0.15	0.998
3[c]	3.44 ± 0.41	0.998
4[d]	2.83 ± 0.15	0.999
5[e]	0.76 ± 0.14	0.999

[a] Global fit result from 10 titrations of p65. [b] Global fit of three titrations shown in Figure 8 for p65 cooperativity analysis. [c] Global fit 10-fold higher concentration of p65/Igκ. [d] Renatured p65. [e] Global fit of p50/Igκ binding (Figure 7).

counts per minute (cpm) [(cpm)total = (cpm)bound + (cpm)-free] and fitting this to the [D]t in each lane. The slope of the linear regression demonstrates the linearity of the signal from the Packard instrument over 3 logs of ^{32}P-labeled Igκ DNA concentration and the effective separation of bound from free DNA by the absence of counts lost to smearing. The second plot (B) of bound IgκB versus total Igκ, a typical binding isotherm, was fit to eq 4 to determine K_d and total active dimer, since we found that allowing the saturation point to float in the regression produces a better fit. This number is referred to as [P]t*. There was no dependence of K_d on the total protein or on the degree of saturation. The regression determines the total dimer concentration to be 6.63 nM, approximating the protein concentration measurements using standard assays (5.22 nM).

For 10 titrations at three different total protein concentrations (at least 3 titrations per [p]t) the error appears random. Once each isotherm was fit separately, a global analysis was performed with the new adjusted [P]t values or [P]t* (see Supporting Information S1: Table 1). This analysis for the p65 homodimer returned a K_d of 4.77 ± 0.21 nM with R^2 = 0.991. This global analysis is within 15% of the value for the same analysis of the three best isotherms, which returns a K_d of 4.11 ± 0.15 nM with R^2 = 0.998 (see Supporting Information S2: Table 2). Also, when each concentration of p65 is raised 10-fold, K_d appears the same as shown in Figure 5 (also see Supporting Information S3: Table 3). Shown in Figure 5 is the global fit normalized to [P]t* and thus saturating at 1:1 stoichiometric ratio of [DB]/[P]t. The same analysis for p50 was performed (Supporting Information S4: Table 4). The three best isotherms fit to the global model with a K_d of 0.76 ± 0.14 nM with R^2 = 0.999 (Figure 6). As can be seen from the tabulated data, the total active protein is at least 80% in most cases. This confirms the stoichiometry of one stable dimer per IgκB duplex for both p50 and p65. To test the possibility of cooperative interactions governing the energetics of Igκ binding to p65, Hill

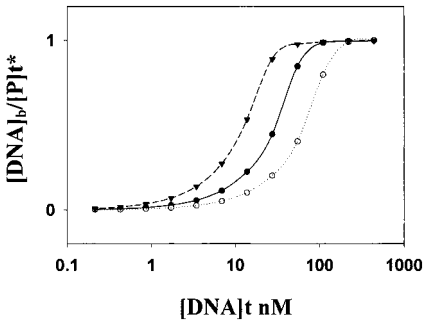

FIGURE 6: Global analysis of binding data for p50: (●) 78.4 nM pt, (○) 156.8 nM pt, and (▼) 39.2 nM pt.

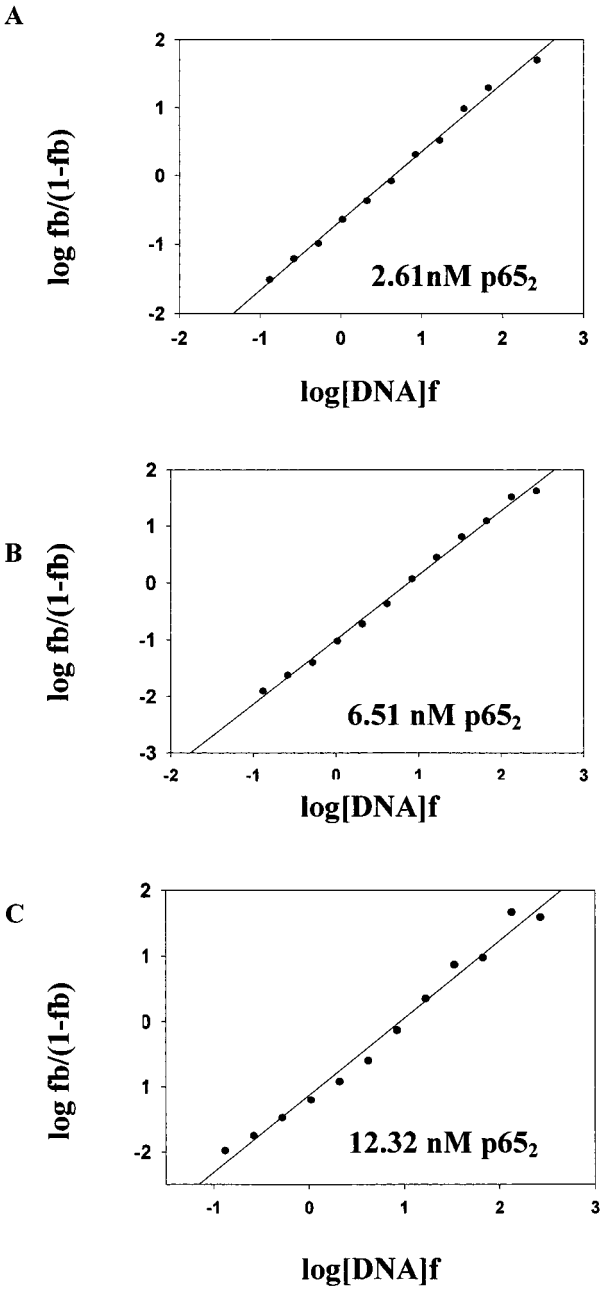

FIGURE 7: Cooperativity analysis of p65/Igκ binding.

plots are shown in Figure 7. Linear regression analysis at the lower concentrations of p65 data generates Hill coefficients of 1. We assume that, with high correlation coefficients (R^2) and a low standard error of our global fits for

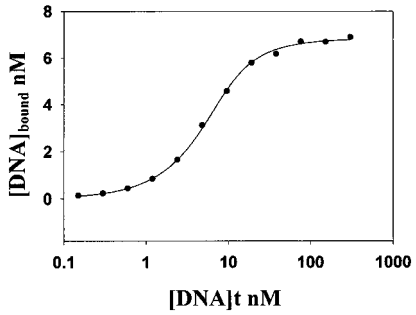

FIGURE 8: Refolding of p65. The p65 NF-κB protein is purified as in Materials and Methods but subjected to an additional denaturation and renaturation scheme. The activity is measured in the standard EMSA (2.83 ± 0.15 nM, R^2 = 0.999 compared to ~4.0 nM, undenatured p65).

data with both p50 and p65, cooperative interactions contributing to the energetics of binding are not significant. Thus, the simple model of a stable protein dimer binding to duplex Igκ with a 1:1 stoichiometry is sufficient to explain all of the binding data. In Table 4, the global fitting results for both p65 and p50 binding to IgκB are summarized.

Refolding of p65. If measures are not taken to remove contaminating bacterial nucleic acids from the recombinant NF-κB preparation, such as lysis in 1 M NaCl buffer, trace amounts of DNA may be significant enough to compete with the labeled, desired Igκ substrate and thus offset the affinity and/or stoichiometry determination. To test this hypothesis, some of the already purified material, with UV spectra as that predicted for a pure protein with p65's composition, was further purified under denaturing conditions. Under these conditions, a cation-exchange resin is expected to bind the protein but not nucleic acids associated with the protein. The denatured p65 bound reasonably well during cation-exchange FPLC with very little absorbance in the flow-through fractions. In a linear gradient from 0 to 1 M NaCl, the protein eluted near 300 mM NaCl and was successfully refolded to obtain active protein. Figure 8 shows the binding isotherm for the renatured p65 binding to IgκB. The K_d for Igκ binding to renatured p65 was not significantly lower than the undenatured, natively purified p65 (2.83 ± 0.15 nM, R^2 = 0.999 compared to ~4.0 nM; Figure 7, Table 4). Thus, if any contaminant exists in the p65 preparation, its effect on binding is negligible. This experiment was not performed with p50 since the calculated and experimental 280/260 ratios were within 2% of each other.

Qualitative Analysis of Enzymatically Synthesized Chiral Phosphoromonothioate-Selected Aptamer Binding. The PCR constructs for thioaptamer selection contain a 22-mer variable region which, in theory, is large enough for two dimers of NF-κB to bind, and further the selected sequences have two "NF-κB-like" 10 bp sequences. Our quantitative binding results presented in the next section, in corroboration with the sequencing results, however, do not indicate that NF-κB has selected for two, tight-binding 10 base pair sites. As a preliminary control experiment, an individual clone from the initial library used in the p50 selection was screened for binding to p50. One clone from the initial library was selected, enzymatically synthesized with monothiophosphate modification 5′ to each dA residue, and purified as described (*27*) and was shown not to bind p50 under the conditions of this experiment (1 nM thioaptamer, 4 nM p50). These

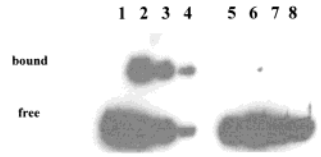

FIGURE 9: Binding of the aptamer clone is influenced by the presence and absence of monothiophosphate modification. Thioaptamer selected by p50 with sulfur (1−4) and without (5−8). Lanes 1 and 5: no p50, 1 nM DNA. Lanes 2−4 and 6−8: $p50_2$ concentration 4 nM. DNA concentration is varied as 0.25, 0.5, and 1 nM. With a 4-fold excess of p50, no binding in lanes 6−8, not thiophosphate modified.

enzymatically synthesized chiral monothiophosphates should have weak affinity for the proteins since there was no combinatorial selection on the library at this point. Furthermore, the presence of ca. 25% phosphorothioate in these initial library clones does not contribute to nonspecific NF-κB binding. Sequences selected from the 20th round of p65 selection at 1 nM show no binding to p50 at 4 nM (data not shown), confirming the specificity of the selection for p65.

To test the importance of the monothiophosphate substitutions in the thioaptamer toward the p50 homodimer, a 15th round clone was PCR synthesized with a nucleotide mix containing dATP instead of dATP(αS). As shown in Figure 9 (lanes 6−8), there appears to be no binding of the normal phosphoryl backbone aptamer under these conditions. This result is similar to the quantitative binding results found for the p65-selected aptamer (see below).

Cold Competition Quantitative EMSA. The aptamer/Igκ competition for NF-κB was performed as described for the uninhibited reaction, the buffer conditions being identical. Each binding experiment was performed at several thioaptamer concentrations, or [I]t, for global nonlinear least-squares fitting. The theoretical model shown here makes use of the classic, competitive inhibition where the binding affinity constant of the protein for its natural substrate, K_d, is modulated by the expression $1 + [I]/K_I$. [I] is free inhibitor concentration and K_I is the dissociation constant of the inhibitor, and a good data fit to this model by regression indicates direct competition between aptamer duplexes and Igκ for the NF-κB DNA binding site.

This quantitative analysis was used to describe the thioaptamer variable region binding of aptamers from the 20th round of the p65 and 15th round of p50 phosphoromonothioate selection. When 22-mers chemically synthesized of the p65 aptamer are compared (thio modified 5′ to each dA) with unmodified phosphoryl duplex, the phosphorothioate binds with at least 3-fold greater affinity than the normal backbone aptamer of the same sequence. The ability of the duplexes to compete against the ^{32}P-labeled Igκ sequence in the standard EMSA is compared. The binding results were fit to the competition model. Table 5 reports the global fitting results for labeled Igκ binding to p65 at three protein concentrations, global fitting at four different concentrations of the normal aptamer duplex (400, 200, 100, and 50 nM all at 25 nM p65), and global fitting results for the phosphoromonothioate-modified aptamer at two concentrations of the duplex (400 and 200 nM at 25 nM p65). The apparent K_d increases and the curve shifts to the right as one goes from uninhibited to normal backbone to phosphorothioate backbone (Figure 10). Plotted in Figure 10 are the normalized to [P]t* curves for the 25 nM p65 titrations which compare uninhibited reactions, the normal backbone aptamer competition reactions, and the thioaptamer competition reactions.

Table 5: Global Fitting Statistics of p65-Selected Thioaptamer Binding to p65 in Cold Competition with Radiolabeled Igκ

		K_d (nM)	R^2	[I]t (nM)	K_i (global)
1[a]	K_d		0.998	0	3.44 ± 0.41
2[b]	K_d^{app}	28.29 ± 0.95	0.999	400	78.85 ± 1.87
3[c]	K_d^{app}	10.8 ± 0.23	0.999	400	249.42 ± 7.16

[a] Global fit of three data sets for uncompeted p65/Igκ reaction. [b] p65/Igκ/thioaptamer reaction. [c] p65/Igκ/phosphoryl aptamer sequence, normal backbone.

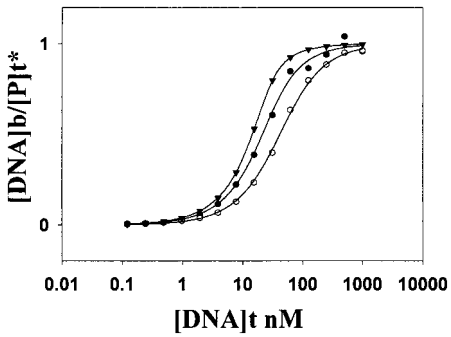

FIGURE 10: Cold competition quantitative EMSA for p65-selected thioaptamers: 1, uninhibited reaction (▼); 2, thiomodified p65-selected sequence (○); 3, unmodified p65-selected sequence (●).

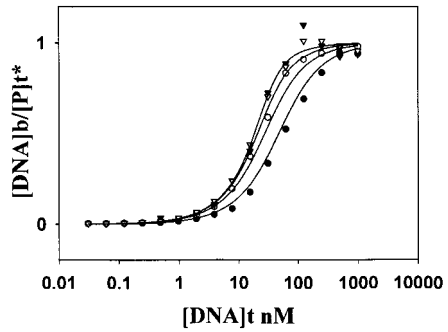

FIGURE 11: Cold competition quantitative EMSA for p50-selected thioaptamers at the indicated thioaptamer concentrations: 800 nM (●), 400 nM (○), 200 nM (▽), and 100 nM (▼).

A similar analysis for the p50-selected aptamer was performed to describe the binding of p50 homodimers to the thioaptamer sequence 6 in Table 3. At a single p50 concentration, four different thioaptamer concentrations were measured for their effect on the p50/Igκ reaction. Plotted in Figure 11 are the binding isotherms of the data normalized to [P]t*. The global analysis was performed once the individual fits returned the saturation plots and a better estimate of total active dimer. Again, as the concentration of thioaptamer increases, the curve shifts to the right and K_d^{app} for Igκ binding increases. Table 6 reports the global fitting results. The global fitting analysis determines a value of 19.6 ± 1.3 nM for the binding of this thioaptamer to p50. It should be noted, however, that each chemically synthesized thioaptamer consists of a diasteromeric mixture containing 2^n different stereoisomers, where n is the number of monothiophosphates ($2^8 = 256$ for the p65-selected aptamer and $2^7 = 128$ for the p50-selected aptamer). The competition assay thus observes the binding of a population of different stereoisomers, not all of which have been selected for. If

Table 6: Results for Chemically Synthesized p50 Selected Aptamer: Igκ/p50 Competition

	K_d (nM)	R^2	[I]t (nM)
1[a]	44.63 ± 1.84	0.999	800
2[b]	11.88 ± 0.66	0.999	400
3[c]	5.16 ± 1.39	0.998	200
4[d]	4.50 ± 0.60	0.997	100
5[e]	19.59 ± 1.25	0.992	global

[a–d] Individual fits at indicated thioaptamer concentrations. [e] Global fit result, all thioaptamer concentrations.

one only considers those thiophosphate modifications in the 10- base thioaptamer binding region of the 22-mer, the numbers reduce to $2^4 = 16$ for the p65-selected thioaptamer and $2^3 = 8$ for the p50-selected thioaptamer. We also observe that since the data fit the global model, the thioaptamers are binding a single NF-κB dimer in a 1:1 stoichiometry.

DISCUSSION

Phelps et al. (*36*) examined the possibility of cooperativity for the cognate mouse NF-κB proteins binding to Igκ. While they also used EMSA to study these interactions, their analysis differs from ours in several ways. To establish a model involving monomer−dimer interactions, they first studied the interaction of dimerization-deficient mutants with a single IgκB half- site. This parameter was utilized in their two parameter fit involving the native proteins. Our analysis of the native proteins only utilizes a single parameter and involves titrating the IgκB site into fixed amounts of native (dimerization active) protein. In this way we were able to measure the stoichiometry as no more than 1 dimer/Igκ duplex. We also found that K_d is independent of protein concentration and Hill plots of the p65 data indicate linearity, with a slope of 1. We therefore limited our analysis to only those conditions where we find an accurate stoichiometry. Under these conditions for both p50 and p65 we were able to perform global fits of our data at six or more protein concentrations for p65 and four for p50, covering at least a 10-fold range for p50 and a 20-fold range for p65. Because our main objective is to measure the binding affinity of our phosphorothioate aptamers to dimers of NF-κB, we limit our competition experiments to only those concentrations where we observe the dimer.

Phosphorothioate aptamer combinatorial selection was performed on the well-characterized human NF-κB proteins. After 20 rounds of selection for p65 and 15 rounds for p50, duplex aptamer sequences resemble known NF-κB sites. The results are compared in Figure 12. Shown are the consensus elements comparing phosphorothioate selection and phosphoryl selection with NF-κB. Kunsch et al. (*11*) performed normal, unmodified binding site selection on recombinant NF-κB homodimers p50 and p65. They were able to demonstrate differential binding; that is, their candidate p50-selected sequence demonstrated higher affinity for p50 than it did for p65 and the p65-selected sequence demonstrated higher affinity for p65 than it did for p50. When comparing the 5′ 10 base pair terminus of the phosphorothioate aptamer sequences to the normal backbone consensus, it is evident that our sequences are altered. Note that the phosphorothioate active binding sequence (A, ii) is the same as the consensus (A, iii) since it occurred most often in our sequencing results

```
                    1234 5 6 7 8 9 10
A   p65   i   5′ GGGR N T T T C C
              CCCY N A A A G G
          ii  5′ GGGG T G T T G T
              CCCC AsC AsAsC As
          iii 5′ GGGG T G T T G T
              CCCC AsC AsAsC As

B   p50   i   5′ GGGG A T T C C C
              CCCC T A A G G G
          ii  5′ GGGG T T C CsA C
              CCCC AsAsG G T G
          iii 5′ GGGA CsA C G R C
              CCCT G T G C Y C
```

FIGURE 12: Selection results for p50 and p65 homodimers. (A) p65-selected (i, PO_4 selection; ii, 5′dSA binding; iii, 5′dSA consensus). (B) p50-selected (i, PO_4 selection; ii, 5′dSA binding; iii, 5′dSA consensus).

from the p65 thioaptamer selection. The p50 consensus sequence (B, iii) and the sequence found to have the tightest binding in our screening of individual clones (B, ii) are different. Thus it is difficult to conclude that there was convergence of the p50 thioaptamer library. At round 10 this sequence was more predominant (4/15 clones). At round 15, 16/22 clones had a similar sequence but failed to show tight binding in the gel shift. It is possible that further rounds of selection would result in convergence of the p50 aptamer library, and in a control experiment, normal backbone aptamer selected as a thioaptamer binds with lower affinity and shows that the thioselection is indeed selecting for thioates in positions that will enhance NF-κB binding. The p65 homodimer is tolerant to changes in positions 4 and 5 (*11*). Note that in position 5 of the p65-thioselected dA(S) there is a T whose complement on the opposite strand is an A residue with 5′ R_p(sulfur) linkage. p50 is the less tolerant of the two homodimers, and the consensus shown (B, i) has no N at any positions or any 5′Y pyrimidine or 5′R for purine. The p50 thioaptamer sequence (B, iii), however, has three substitutions at positions 5, 6, and 9 where the T in position 6 is unchanged. The T in position 5 of both thio-selected sequences has been altered, even with p50. It is possible that significant distortion of the duplex by the monthio's or the selective interaction of the thioate with the protein contributes to this. The nonbinding clones from the initial libraries, Tables 2 and 3, sequence 15, which have thio modification, have no sequence resemblance to the NF-κB sites, nor do they demonstrate binding affinity for NF-κB. Nowhere in these sequences is there a 4-base polyG tract as seen with the natural binding sites and with the thio-selected aptamers, suggestive that this motif is of critical importance, regardless of sulfur. Furthermore, these molecules are shown to not bind NF-κB where under identical conditions the selected sequences do bind.

Currently underway are the enzymatic synthesis of R_p phosphorothioates which has been described in the literature (*37*, *38*). These syntheses are currently being reproduced in our laboratory. It will be important to know the energetic effects of stereochemistry on binding to our thioaptamers since this is the precise R_p aptamer stereochemistry selected for. Using the quantitative methodologies for the measurement of thioaptamer binding to NF-κB presented here will enable us to observe the energetic differences between R_p or S_p modification. We predict that the R_p configured thioaptamers will bind more tightly to NF-κB since this is the precise stereochemistry selected for. This prediction is

based on the observed high-affinity binding of the PCR synthesized thioaptamers, which are stereochemically pure, and also the binding results observed in the absence of the R_p modification where relatively weak affinity is observed. The electrostatic and size properties of sulfur atoms and their effect on the duplex structure will determine the contacts with interacting amino acid residues in the protein. This will be important when elucidating the crystal structure of the thioaptamer in complex with NF-κB.

In conclusion, we have shown that thioaptamers with high affinity for p65 and p50 NF-κB dimers can be selected for both base sequence and backbone substitution. The sulfur substitution enhances the binding relative to the same sequence with normal backbone. The sulfur substitution also alters the sequence that is obtained by in vitro combinatorial selection. Postselection phosphorothioate modifications of the in vitro combinatorially selected sequence can thus result in aptamers in which affinity cannot be reliably predicted. The simultaneous selection for both avoids this difficulty.

ACKNOWLEDGMENT

We thank the following people for technical consultations: Judy Aronson for selection methodologies and Bo Xu for protein purification.

SUPPORTING INFORMATION AVAILABLE

Tabulated results of NF-κB and IgκB binding data (see text). This material is available free of charge via the Internet at http://pubs.acs.org.

REFERENCES

1. Gold, L., Polisky, B., Uhlenbeck, O., and Yarus, M. (1995) *Annu. Rev. Biochem. 64*, 763.
2. Aurup, H., Williams, D. M., and Eckstein, F. (1992) *Biochemistry 31*, 9636.
3. Shuker, S. B., Hajduk, P. J., Meadows, R. P., and Fesik, S. W. (1996) *Science 274*, 1531.
4. Tuerk, C., and Gold, L. (1990) *Science 249*, 505.
5. Ellington, A. D., and Szostak, J. W. (1992) *Nature 355*, 850.
6. Ellington, A. D., and Szostak, J. W. (1990) *Nature 346*, 818.
7. Famulok, M., and Mayer, G. (1999) *Curr. Top. Microbiol. Immunol. 243*, 123.
8. Hermann, T., and Patel, D. J. (2000) *Science 287*, 820.
9. Miyamoto, S., and Verma, I. M. (1995) *Adv. Cancer Res. 66*, 255.
10. Baldwin, A. S., Jr. (1996) *Annu. Rev. Immunol. 14*, 649.
11. Kunsch, C., Ruben, S. M., and Rosen, C. A. (1992) *Mol. Cell. Biol. 12*, 4412.
12. Ghosh, S., May, M. J., and Kopp, E. B. (1998) *Annu. Rev. Immunol. 16*, 225.
13. Siebenlist, U., Franzoso, G., and Brown, K. (1994) *Annu. Rev. Cell Biol. 10*, 405.
14. Karin, M. (1998) *Cancer J. Sci. Am. 4* (Suppl. 1), S92.
15. May, M. J., and Ghosh, S. (1998) *Immunol. Today 19*, 80.
16. Beg, A. A., Sha, W. C., Bronson, R. T., Ghosh, S., and Baltimore, D. (1995) *Nature 376*, 167.
17. Doi, T. S., Takahashi, T., Taguchi, O., Azuma, T., and Obata, Y. (1997) *J. Exp. Med. 185*, 953.
18. Caldenhoven, E., Liden, J., Wissink, S., Van de Stolpe, A., Raaijmakers, J., Koenderman, L., Okret, S., Gustafsson, J. A., and Van der Saag, P. T. (1995) *Mol. Endocrinol. 9*, 401.
19. Sen, C. K., Traber, K. E., and Packer, L. (1996) *Biochem. Biophys. Res. Commun. 218*, 148.
20. Umezawa, K., Ariga, A., and Matsumoto, N. (2000) *Anti-Cancer Drug Des. 15*, 239.
21. Cummins, L., Graff, D., Beaton, G., Marshall, W. S., and Caruthers, M. H. (1996) *Biochemistry 35*, 8734.
22. Milligan, J. F., and Uhlenbeck, O. C. (1989) *Biochemistry 28*, 2849.
23. Marshall, W. S., and Caruthers, M. H. (1993) *Science 259*, 1564.
24. Brukner, I., and Tremblay, G. A. (2000) *Biochemistry 39*, 11463.
25. Lewis, J. G., Lin, K. Y., Kothavale, A., Flanagan, W. M., Matteucci, M. D., DePrince, R. B., Mook, R. A. J., Hendren, R. W., and Wagner, R. W. (1996) *Proc. Natl. Acad. Sci. U.S.A. 93*, 3176.
26. Wagner, R. W., and Flanagan, W. M. (1997) *Mol. Med. Today 3*, 31.
27. King, D. J., Ventura, D. A., Brasier, A. R., and Gorenstein, D. G. (1998) *Biochemistry 37*, 16489.
28. Andreola, M. L., Calmels, C., Michel, J., Toulme, J. J., and Litvak, S. (2000) *Eur. J. Biochem. 267*, 5032.
29. Cho, Y., Zhu, F. C., Luxon, B. A., and Gorenstein, D. G. (1993) *J. Biomol. Struct. Dyn. 11*, 685.
30. Kurpiewski, M. R., Koziolkiewicz, M., Wilk, A., Stec, W. J., and Jen-Jacobson, L. (1996) *Biochemistry 35*, 8846.
31. Koziolkiewicz, M., Owczarek, A., and Gendaszewska, E. (1999) *Antisense Nucleic Acid Drug Dev. 9*, 171.
32. Zhang, Y. L., Hollfelder, F., Gordon, S. J., Chen, L., Keng, Y. F., Wu, L., Herschlag, D., and Zhang, Z. Y. (1999) *Biochemistry 38*, 12111.
33. Brody, E. N., Willis, M. C., Smith, J. D., Jayasena, S., Zichi, D., and Gold, L. (1999) *Mol. Diagn. 4*, 381.
34. Smith, J. S., and Nikonowicz, E. P. (2000) *Biochemistry 39*, 5642.
35. Thiesen, H. J., and Bach, C. (1990) *Nucleic Acids Res. 18*, 3203.
36. Phelps, C. B., Sengchanthalangsy, L. L., Malek, S., and Ghosh, G. (2000) *J. Biol. Chem. 275*, 24392.
37. Eckstein, F. (2000) *Antisense Nucleic Acid Drug Dev. 10*, 117.
38. Stec, W. J., Grajkowski, A., Koziolkiewicz, M., and Uznanski, B. (1991) *Nucleic Acids Res. 19*, 5883.

BI020220K